Hydrazide-based organogels and liquid crystals with columnar order

Binglian Bai, Haitao Wang, Hong Xin, Fenglong Zhang, Beihong Long, Xiaobing Zhang, Songnan Qu and Min Li*

Received (in Montpellier, France) 4th October 2006, Accepted 5th January 2007
First published as an Advance Article on the web 2nd February 2007
DOI: 10.1039/b614444f

We report on the synthesis and self-assembly of a new series of compounds containing a hydrazide unit in the rigid core and three alkoxy chains with varying lengths. The compounds *N*-(3,4,5-cetyloxybenzoyl)-*N*′-(4′-nitrobenzoyl) hydrazine (**C16**) and *N*-(3,4,5-dodecyloxybenzoyl)-*N*′-(4′-nitrobenzoyl) hydrazine (**C12**) exhibited stable columnar phase and strong gelation ability in several apolar organic solvents. The columnar structure was found both in the liquid crystalline state and in the xerogels by wide-angle X-ray diffraction analysis. SEM and TEM images revealed that the molecules self-assembled into twist fibrous aggregates in the xerogels. FT-IR and ^{1}H NMR studies confirmed that the intermolecular hydrogen bonding and van der Waals interactions were the major driving force for the formation of self-assembling both the liquid crystals and gels processes. Further detailed analysis of their aggregation modes were conducted by FT-IR spectroscopy and X-ray diffraction measurement.

Introduction

Self-assembling processes are common throughout nature and technology.[1] Self-assembled materials, such as liquid crystals and organogels, formed by non-covalent bonding have attracted much attention because they are good candidates for the next generation of materials, for which dynamic function, environmental benignity, and low energy processing are required.

The liquid crystalline state represents fascinating states of soft matter combining order and mobility on a molecular and supra-molecular level.[2,3] The organogels are a class of nano-structured materials composed of a self-assembled superstructure of the low molecular weight organogelators through specific intermolecular interactions and a large volume of organic liquid immobilized therein.[4] In order for these self-assemblies to form, it is important to control the intermolecular interactions in such a way that they enable the formation of liquid crystals and organogels, but avoid transformation to a crystalline state. It is relatively rare to find low molecular rod-like compounds capable of both gelling solvents and exhibiting thermotropic mesomorphic behaviors, whereas this is the usual case for some wedge-shape or disk-like molecules.[5]

Among those non-covalent interactions, hydrogen bonding was most commonly used to direct the self-assembling process. Many low molecular weight organogels, containing, for example, amide,[6–10] urea,[9–11] and hydrazide[12] groups have been reported to show strong gelation ability in organic solvents, and where the intermolecular hydrogen bonding was considered to be the driving force. Although it has been known that intermolecular hydrogen bonding played an important role in mesophase formation in the dihydrazide derivatives; for example, linear *N*,*N*′-bis(4-alkoxybenzoyl) hydrazines exhibit a cubic phase,[13,14] while monomeric, dimeric and polymeric *N*,*N*′-bis[3,4,5-tris(alkoxybenzoyl)] hydrazines formed a columnar phase,[14,15] little attention has been paid to organogels based on dihydrazide derivatives. Recently, our groups have demonstrated that intermolecular hydrogen bonding was still interacting in the SmA phase and played important roles in stabilizing the mesophase and organogels of dihydrazide derivatives.[16–18]

In this context, a series of low molecular compounds containing of dihydrazide groups were designed. Notably, the compounds showed thermotropic mesophase and strong gelation ability in organic solvents, and the twist fibers were observed, which was due to the steric hindrance and hydrogen bonding interactions between the dihydrazide groups co-operating with the packing of the alkoxy chains instead of any chiral groups. Both the length of the alkyl chains and the existence of hydrogen bonding can strongly influence the properties of the mesophase and organogels.

Results and discussion

Synthesis of compounds

The compounds were synthesized according to the route shown in Scheme 1. 4-Nitrobenzoyl chloride was reacted with 3,4,5-alkoxy-benzoylhydrazine in THF, yielding the products of compounds **C***n*. The molecular structure of **C***n* was confirmed by the disappearance of the protons of the $-NH_2$ group at about 4.4 ppm from 3,4,5-alkoxy-benzoylhydrazine and the appearance of two different ones from the –NH groups at upwards of 9.0 ppm. In order to investigate the hydrogen bonding effect on the behaviour of liquid crystals and gel ability, compound Me–**C16** was prepared in which the hydrogens of dihydrazide group of **C16** were substituented by methyl. The disappearance of N–H stretching vibrations (ν(N–H)) of **C16** at 3187 cm^{-1} clearly indicated the proposed

Key Laboratory for Automobile Materials(JLU), Ministry of Education, Institute of Materials Science and Engineering, Jilin University, Changchun, 130012, P. R. China. E-mail: minli@mail.jlu.edu.cn

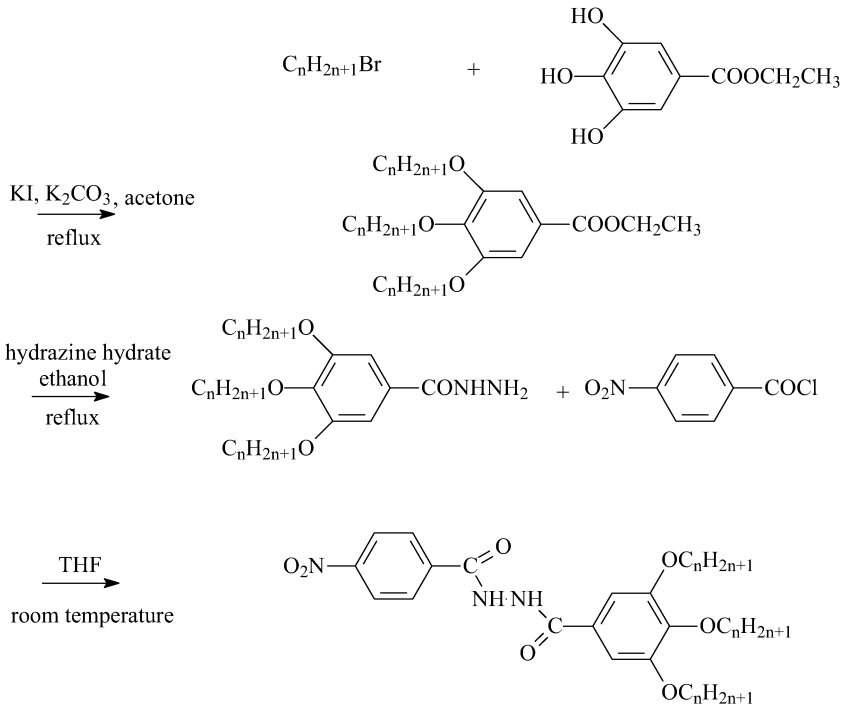

Cn n=3, 12, 16

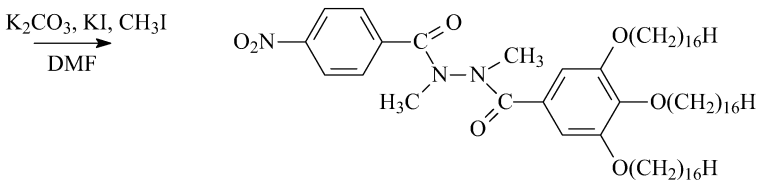

Me-C16

Scheme 1 The synthesis of compound **C***n* and Me–**C16**.

molecular structure of Me–**C16**. Detailed characterization data for **C***n* and Me–**C16** were given in experimental section.

Intermolecular hydrogen bonding in C*n*

In order to explore the hydrogen bonding motif, temperature dependent FT-IR and concentration dependent ^{1}H NMR spectroscopic experiments were performed. In the ^{1}H NMR dilution studies, the amide protons of compounds **C***n* showed a strong concentration dependence, for example, reducing the concentration of **C3** in $CDCl_3$ from 104 to 0.033 mM causes both NH-1 (near to nitro phenyl, $\Delta\delta$ = 1.405 ppm) and NH-2 (near to alkoxy phenyl, $\Delta\delta$ = 0.841 ppm) to shift upfield remarkably (Fig. 1), which strongly indicates that both the two amide protons in **C3** participate in forming supramolecules *via* cooperative double intermolecular hydrogen bonds.[19] The data from the diluting experiment fit well with the calculated curves using the simplest (isodesmic) model (*i.e.*, $K_n = K$, for $n \geq 2$),[20] giving association constants (K) of 81.3 M^{-1} and 62.1 M^{-1} based on NH-1 and NH-2, respectively.

Intermolecular hydrogen bonding in **C***n* was further confirmed by temperature dependent FT-IR spectroscopy. Table 1 presented the assignments of infrared frequencies for **C12**.[16,21] The presence of –N–H stretching vibrations at 3193 cm^{-1} (the absence of free ν(N–H), which exhibits a relatively sharp band at around 3400 cm^{-1}), intense absorption of amide I at 1662, 1594 cm^{-1} clearly indicated that almost all the –NH groups are associated with –C=O groups *via* –C=O···H–N– hydrogen bonding.[16,22]

Moreover, these conclusions were supported by the fact that the ν(N–H) became weaker and shifted to higher frequencies as well as the hydrogen bonding length[23,24] of –C=O···H–N– increasing upon heating, as shown in Fig. 2. The wavenumbers of ν(N–H) of **C12** are at around 3193, 3216 and 3277 cm^{-1} in the crystalline state, Col phase and isotropic phase, respectively, and apart from the main band at 3277 cm^{-1}, a shoulder peak appeared at 3395 cm^{-1} (free ν(N–H)) in isotropic phase. The calculated hydrogen bonding length of –C=O···H–N– was 2.00 Å at 30 °C, which is in the range of moderate hydrogen bonds.[24] It increased slowly with temperature within the crystalline and columnar phase, while jumped to 2.18 Å, which indicated a weak hydrogen bonding in the isotropic state.[24] The integral intensity of ν(N–H) increases strongly upon formation of a hydrogen bond, and this is often taken as

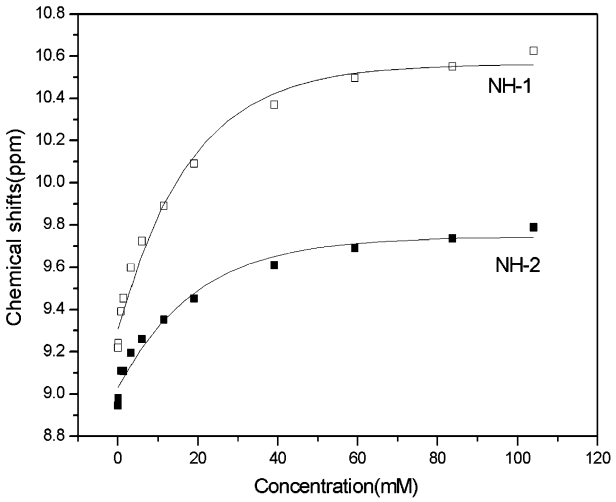

Fig. 1 The chemical shifts of amide protons for **C3** *vs.* concentrations in $CDCl_3$ (NH-1: near to nitro phenyl, NH-2: near to alkoxy phenyl).

a more reliable indicator of hydrogen bond formation.[24] The integral intensity of the ν(N–H) (Fig. 2b) of **C12** decreased slowly near the melting temperature, and it decreased drastically upon isotropic transition (Ti) and remained more or less constant above Ti. The reason for this decrease in the intensity of ν(N–H) can be ascribed to the increased mobility of the system. In a word, changes of both the intensity and wavenumber of ν(N–H) and the increase of hydrogen bonding length of –C═O···H–N– with temperature strongly indicated that the presence of the intermolecular hydrogen bonding in the Col phase of **C12**.[14] Furthermore, this conclusion was also supported by the fact that the –C═O stretching vibrations shifted from 1662, 1594 cm^{-1} to 1691, 1646 cm^{-1}, and a sharp decrease of the absorption intensity at columnar–isotropic transition (Fig. 3). All these demonstrated that there were moderate hydrogen bonding between –C═O and –N–H in the liquid crystalline state of **C***n*, and the intermolecular hydrogen bonding was very important for the stabilization of the columnar phase.

Thermotropic mesomorphic behaviour of the C*n* and Me–C16

The thermotropic properties of **C***n* and Me–**C16** were investigated by a combination of DSC, POM and XRD. Their transitional temperatures and associated enthalpies were summarized in Table 2. No mesophase was observed in **C3**, whereas the compounds **C12** and **C16** showed enantiotropic columnar liquid crystalline phases. The melting points decreases and the mesophase appears with the elongating terminal chains. This may be explained as the elongation of the terminal chains increased the micro-segregation effect by enhancing the incompatibility between the hydrogen bonded rigid aromatic rings and flexible alkoxy chains. On the other hand, melting point of Me–**C16** decreased nearly 15 °C compared to that of **C16** and no mesomorphic phase was observed in Me–**C16**.

Table 1 Assignments of infrared frequencies for **C12** at room temperature

IR frequencies (cm^{-1})	Assignments
3193	ν(N–H)
2956	$\nu_{as}(CH_3)$
2922	$\nu_{as}(CH_2)$
2871	$\nu_s(CH_3)$
2851	$\nu_s(CH_2)$
1662, 1594	Amide I, ν(C═O)
1610, 1581, 1566	ν(C═C) of phenyl ring
1492	Amide II, III, $\nu_{C-N} + \delta_{N-H}$
1525, 1342	ν_{as}, $\nu_s(NO_2)$
1466, 1456	$\delta(CH_2)$
1229	ν(Ar–O)
1123	ν(C–O)
719	$(CH_2)_n$ rocking modes, $n \geq 4$

Compound **C12** exhibits a ribbon-like texture coexistence with a spherulitic one, while no characteristic texture was observed for **C16** under POM. X-ray diffraction measurements of **C***n* have been performed across a wide temperature range in their mesophases. The X-ray diffraction pattern of **C12**, as shown in Fig. 4a, taken at 130 °C revealed a hexagonal columnar structure with the column diameters of 31.45 (100), 18.17 (110), 15.62 Å (200) in the low angle region with a reciprocal spacing ratio of $1 : 1/\sqrt{3} : 1/2$. Table 3 lists the *d*-spacings (Å) and the corresponding Miller indices shown in the graph in Fig. 4a. The estimated all-*trans* molecular length of the most extended conformation of **C12** is 28.83 Å, obtained by the MM2 method, and the diameter of a column of the columnar phase is 36.32 Å. The number of molecules within one disk was calculated to be four,[4b,25] assuming that the density of **C12** is 1 g cm^{-3}. Thus, the alkoxy chains can effectively surround the polar (nitro) part and a circular shape of the columns can be assumed and the four molecules distribute the disk averagely. Likewise, X-ray diffraction measurements of **C16** was performed and displayed in Fig. 4b and Table 3. The calculated spacings, shown in Table 3, were obtained after fitting the experimentally observed spacings to a monoclinic unit cell, where the best fit for the data was obtained for a rectangular cell with dimensions a = 110.62 Å and b = 45.05 Å. Thus, the compound **C16** shows a rectangular columnar cell. The calculated molecular length of **C16** is 34.75 Å, obtained by the MM2 method, and the value of a, b of a column of the columnar phase is in reasonable agreement with the calculated molecular length. The number of molecules within a slice was calculated to be six,[4b,25] assuming that the density of **C16** is 1 g cm^{-3}, the packing model for the rectangular column is shown in Fig. 4c.

Gelation

Interestingly, only **C12** and **C16** with long alkyl chains and intermolecular hydrogen bonding showed strong gelation ability in organic solvents such as benzene, 1,2-dichloroethane *et al.* No gelation is observed for compounds **C3** and Me–**C16** in which the hydrogen of dihydrazide group of **C16** were replaced by methyl groups. Table 4 lists the minimum gelation concentrations (MGC) of **C12** and **C16** in organic solvents. It can be seen that **C16** gelator is more efficient than **C12**. Fig. 5 shows the melting temperature (T_m) of benzene gel based on **C12** as a function of concentration. T_ms were determined by the "falling drop" method.[26] The T_m increases from 27 °C to 41 °C as the concentration of **C12** increase from 1.02 wt% to 4.90 wt%.

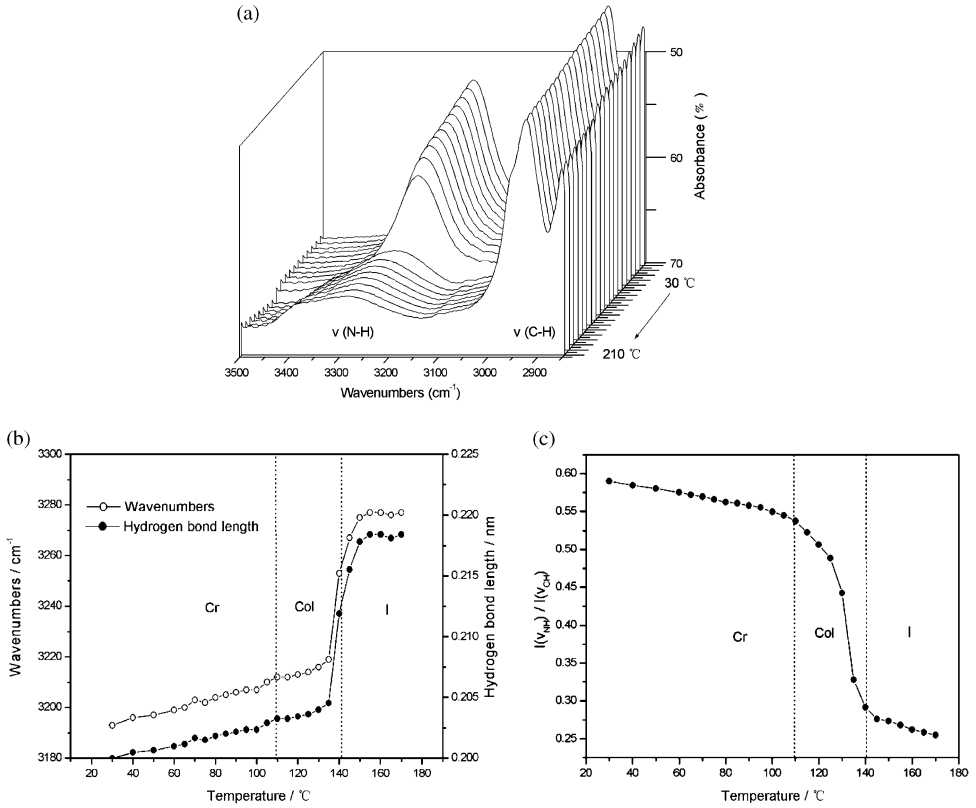

Fig. 2 (a) The temperature dependent FT-IR spectra of **C12** at an interval of 10 °C in the range of 3500–2800 cm^{-1}, the plot of (b) ν(N–H) wavenumbers and hydrogen bond length of –C═O···H–N– of **C12** *vs.* temperature and (c) integral intensity of ν(N–H) of **C12** *vs.* temperature.

Self-assembled behaviours of the organogels

In order to investigate the aggregation morphology of these organogels, the xerogels were prepared and subjected to the SEM observation. Fig. 6a showed the SEM image of **C12** xerogels from benzene that revealed a network structure composed of twist bundles of fibers. The diameter of each bundle was found to be 300–400 nm, juxtaposed and intertwined by several long slender aggregations with the diameter of *ca.* 150–200 nm. While the SEM image of a benzene gel of **C16** reveals a number of bundles of fibers, similar to that of **C12** with the diameter of *ca.* 100 nm. Xerogels of **C12** and **C16** from toluene and 1,2-dichloroethane exhibited the similar SEM images to that from benzene. The self-assembled twisted fibers with the diameter of *ca.* 100 nm of **C16** were also clearly observed by the TEM even in the homogeneous fluid benzene solution (0.13 wt%) (Fig. 6c and d), but the twist can only be seen on a few fibers, many straight fibers were observed. It is possible that the steric hindrance decreases and the free energy increases in the homogeneous fluid solution.

To reveal the packing conformations of the molecules in gel phase, X-ray diffraction was measured. The XRD pattern (as seen in Fig. 7a) of benzene xerogels (2.802 wt%) of **C12** consists of seven peaks at 55.85 (200), 30.32 (110), 14.28 (420), 9.46 (530), 7.22 (440), 5.71 (550), 4.20 (001) Å, which correspond to a rectangular columnar packing (a = 111.70 Å, b = 31.50 Å). Based on these observations, we propose that columns assemblies with rectangular lattice parameters to

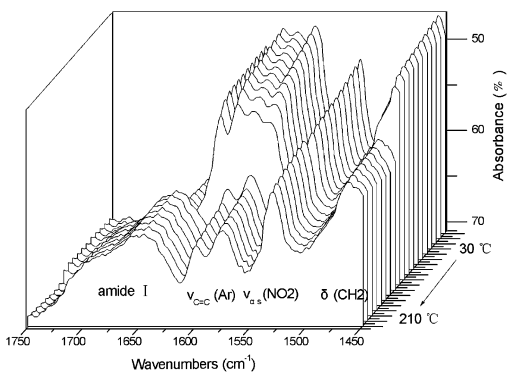

Fig. 3 The temperature dependent FT-IR spectra of **C12** at an interval of 10 °C in the range of 1750–1450 cm^{-1}.

Table 2 Phase behaviour of compounds of **C***n* and Me–**C16**[a]

Compound	T/°C(ΔH/kJ mol^{-1})
C3	Cr 177.9 (37.23) I
C12	Cr 109.0 (13.70) Col_h 142.0 (37.19) I
C16	Cr 111.2 (40.61) Col_r 135.2 (45.21) I
Me–**C16**	Cr 95.8 (99.11) I

[a] The transitional temperatures and enthalpies (in parentheses) were determined by DSC (10 °C/min). Cr indicates a crystalline phase, Col_h indicates a hexagonal columnar phase, Col_r indicates a rectangular columnar phase and I indicates an isotropic phase.

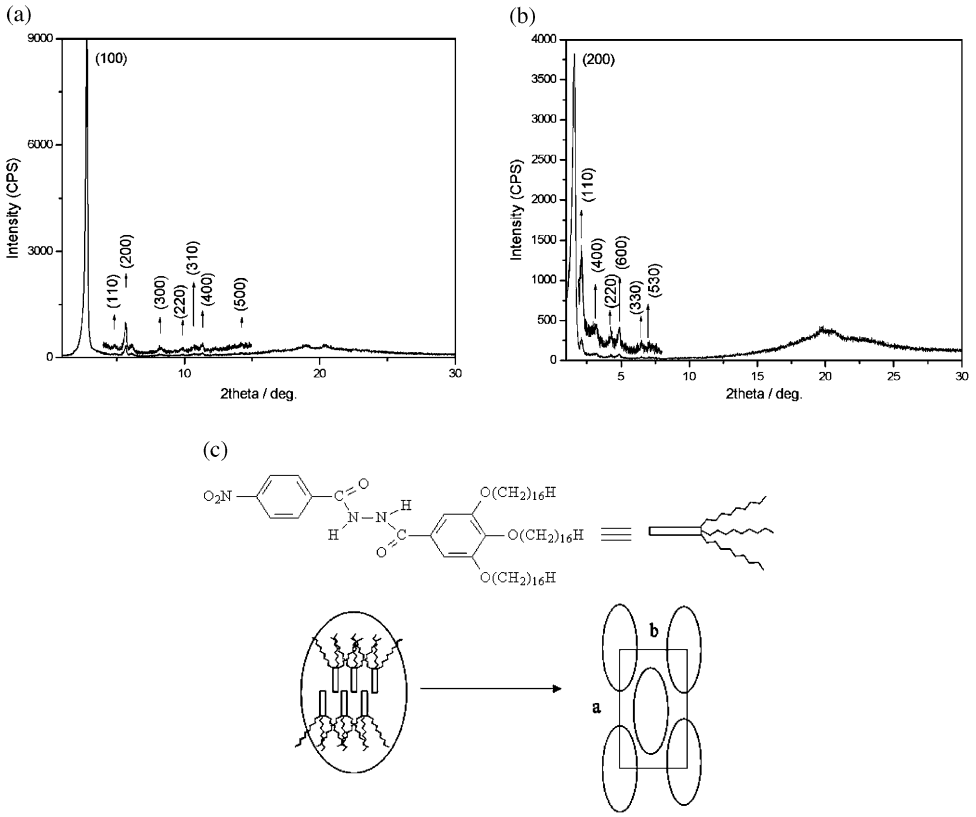

Fig. 4 XRD of (a) **C12** at 130 °C, (b) **C16** at 125 °C and (c) the packing model for the rectangular column of **C16**.

make elementary fibers. Each bundle with the diameter of 300–400 nm can be thought to consist of 30–40 elementary fibers, which are visible by SEM. When the length of the alkoxy chains increased (**C16**), the self-assembled structures changed from rectangular to hexagonal packing with the spacings of 56.56 (100), 32.32 (110), 28.01 Å (200) in the small-angle regions, with a reciprocal spacing ratio of 1 : $1/\sqrt{3}$: 1/2 (Fig. 7b). The diameter of a column of the hexagonal packing is 65.31 Å, namely the diameter of elementary fibers. Each bundle with the diameter of 100 nm can be thought to consist of *ca.* 15 elementary fibers, as shown in Fig. 6b.

The formation of elongated fiber-like aggregates indicates that the self-assembly of **C***n* is driven by strong directional intermolecular interactions. To ascertain whether hydrogen bonding plays a role in the gelation process, infrared spectrum of the **C12** organogel was examined. The presence of –N–H stretching vibrations at 3184 cm^{-1} and –C═O stretching vibrations at 1665 cm^{-1} and 1593 cm^{-1} for **C12** in the gel state unambiguously suggested that the hydrogen bonding through –N–H···O═C– exists in the gelation process. The hydrogen bonding was confirmed to be the intermolecular one through the ^{1}H NMR studies (*vide supra*), and it is confirmed that the compound Me–**C16** did not gel organic solvent. These results strongly indicated that –N–H groups were exclusively involved in intermolecular hydrogen bonding[19,27] and play an important role in the gelation process. Furthermore, the absorption bands of the antisymmetric (ν_{as}) and symmetric (ν_s) –CH_2– stretching vibrational modes of **C12** are observed

Table 3 XRD data for the liquid crystalline phases of **C12** and **C16**

Compound	*T*/°C	Phase	*d*, (obsd)/Å	*d*, (calcd)/Å	Miller index
C12	130	Col_h a = 36.32	31.45	31.45	100
			18.17	18.16	110
			15.62	15.73	200
			14.53	—	—
			10.72	10.48	300
			8.97	9.08	220
			8.30	8.72	310
			7.79	7.86	400
			6.23	6.29	500
			4.66	4.54	440
			4.35	—	001
C16	125	Col_r	55.31	55.31	200
		a = 110.62	41.72	41.72	110
		b = 45.05	27.76	27.56	400
			20.68	20.85	220
			18.17	18.37	600
			13.64	13.90	330
			12.58	12.41	530
			4.03	—	001

Table 4 Minimum gel concentrations (MGC) of **C12** and **C16**

	MGC (wt%)	
Solvent	**C16**	**C12**
Benzene	0.280	0.686
Toluene	0.305	0.590
1,2-dichloroethane	0.105	0.173
Chloroform	Solution	Solution

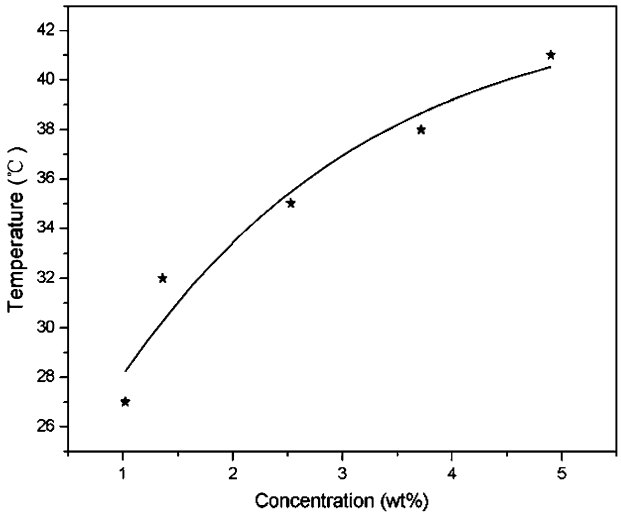

Fig. 5 Concentration-dependent melting temperature of gels based on **C12** in benzene.

at 2924 cm^{-1} (ν_{as} –CH), 2854 cm^{-1} (ν_s –CH) in $CHCl_3$ solution, while they shift to 2921 and 2850 cm^{-1} in the benzene gel, respectively. The red-shift reveals a decrease in the fluidity of the alkyl chains due to the strong organization of the alkyl groups *via* a van der Waals interaction.[28] Consequently, the driving forces for organogelation followed by entanglement of the self-assembled nanofibers are mainly hydrogen bonding and van der Waals interactions.

Combining the above results from the FT-IR and XRD data, the reason for the generation of the twisted fibers from achiral molecules could be deduced. In the process of gelation, the hydrogen bonding, π–π and the van der Waals interactions arranged the molecules to aggregate into fibrous structure. Combination the steric hindrance and hydrogen bonding interactions between the dihydrazide groups effects some degree rotation of the phenyl. Therefore the disks would be aggregated in a propeller-like conformation, which might provide an induction for the formation of twist. And the slightly disordered packing of the alkoxy chains (the absence of sharp peaks in the wide-angle region for XRD data) induced the formation of twist propeller-like conformations and gave macroscopic twisted structures. All of above results indicate that both the steric hindrance and hydrogen bonding interactions between the dihydrazide groups as well as the packing of the alkoxy chains are critically important to form the twist fibers in this series of compounds.

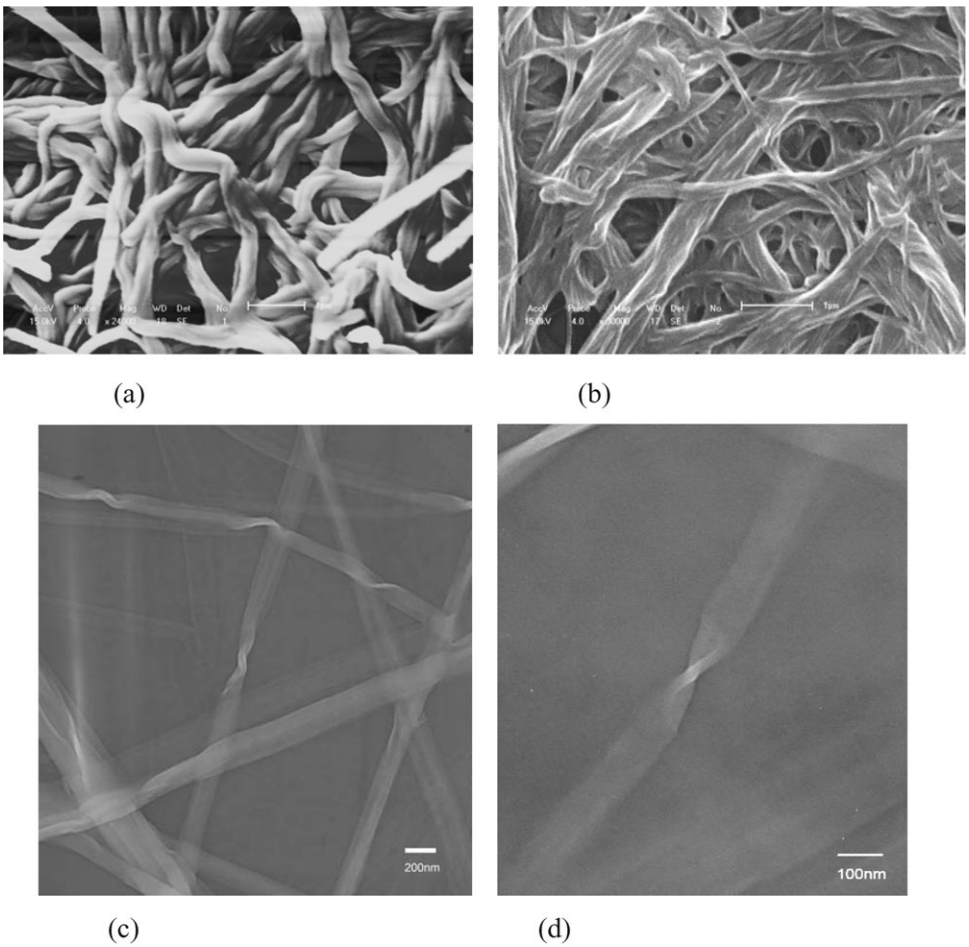

Fig. 6 (a) SEM image of xerogel from **C12** in benzene (2.802 wt%), (b) SEM image of xerogel from **C16** in benzene (0.607 wt%), (c, d) TEM image of the benzene solution of **C16** (0.13 wt%).

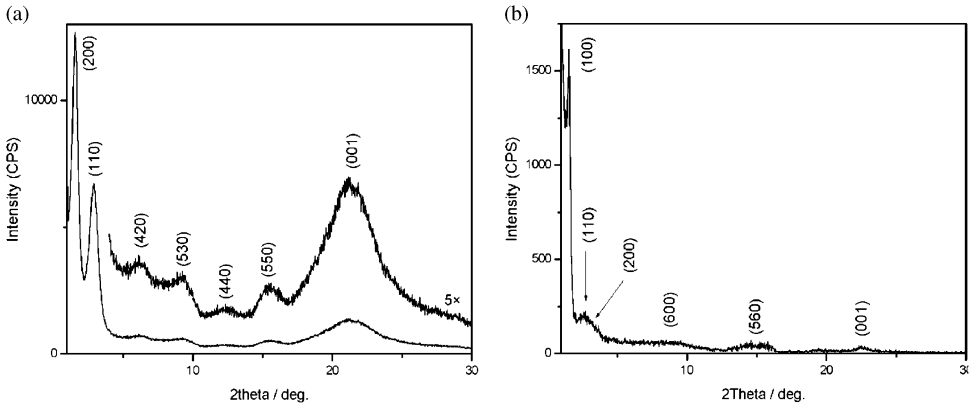

Fig. 7 X-Ray diffraction pattern of the benzene xerogels of (a) **C12** (2.802 wt%) and (b) **C16** (0.607 wt%).

Conclusion

In conclusion, a new series of achiral compounds containing a dihydrazide unit in the rigid core was designed. We demonstrated the unique self-assembling ability of the compounds **C12** and **C16**, which showed stable thermotropic Col phase and strong gelation abilities. The columns assemblies were found both in the liquid crystalline state and in the xerogels. Intermolecular hydrogen bonding between the dihydrazide groups and van der Waals interactions between the alkyl chains were demonstrated to be the major driving force for both self-assembling processes. The formation of the twist fibers was due to the steric hindrance and hydrogen bonding interactions between the dihydrazide groups cooperating with the packing of the alkoxy chains.

Experimental

Synthesis

All commercially available chemicals were of reagent grade and were used without further purification. 3,4,5-trihydroxy benzoic acid ethyl ester and 1-bromide alkyl were purchased. 3,4,5-Trialkoxy-benzoyl hydrazine was prepared according to literature procedures.[29] Alcohol used for recrystallization is anhydrous and alcohol content is more than 99.7%. The compounds were synthesized according to the route shown in Scheme 1.

Gelation experiments

The weighted powder compound and solvent were sealed in a little glass tube, and were then gently heated to make the gelator completely dissolved. The resulting solution was cooled in air or ice–water bath (in the low concentration case) for several minutes, and then the gelation was checked visually. When upon inversion of the test tube no fluid ran down the walls of the tube, we judge it ''gelation''. The xerogels were obtained through slowly evaporating the solvents from organogels, which were kept in the air at about 4 °C.

Experimental technique

^{1}H NMR spectra were recorded with a Bruker Avance 500 MHz spectrometer, using chloroform-*d* as solvent and tetramethylsilane (TMS) as an internal standard. FT-IR spectra were recorded with a Perkin–Elmer spectrometer (Spectrum One B). The sample was pressed tablet with KBr. The thermal properties of the compounds were investigated with a Mettler-Toled. DSC821^e instrument. The rate of heating and cooling was 10 °C min^{-1}; the weight of the sample was about 2 mg, and indium and zinc were used for calibration. The peak maximum was taken as the phase transition temperature. Optical textures were observed by polarizing optical microscopy (POM) using a Leica DMLP microscope equipped with a Leitz 350 heating stage. X-Ray diffraction was carried out with a Bruker Avance D8 X-ray diffractometer. T_ms were determined by the ''falling drop'' method. An inverted gel was immersed in a water bath initially at or below the room temperature. The water was heated slowly until T_m, the temperature at which the gel fell due to the force of gravity. SEM observations were taken with a SSX-550 apparatus. Samples for SEM study were xerogels. Transmission electron microscopy (TEM) morphology was obtained with JEM 2010 apparatus. Samples for TEM study were prepared by dropping small amount of solution onto a 400-mesh copper grid following by natural evaporating the solvent.

N-(3,4,5-Propyloxybenzoyl)-*N*′-(4′-nitrobenzoyl) hydrazine (C3)

3,4,5-tripropyloxy-benzoylhydrazine (1.96 g, 4.26 mM) and 4-nitrobenzoyl chloride (0.79 g, 4.26 mM) were dissolved in tetrahydrofuran (100 ml), pyridine (2 ml) was added, and the resulting mixture was stirred at room temperature for 8 h. The reaction mixture was poured into an excess of ice water, and the precipitate recrystallized from anhydrous alcohol; yield 64.5%. Compounds **C12** and **C16** were synthesized according to the same procedure.

δ_H (500 MHz; $CDCl_3$; Me_4Si): 10.50 (s, 1H), 9.69 (s, 1H), 8.19 (d, 2H, J = 8.4 Hz), 8.00 (d, 2H, J = 8.3 Hz), 7.04 (s, 2H), 3.98–3.89 (m, 6H), 1.78 (m, 6H), 1.02 (td, 9H, J = 7.3 Hz, J = 14.8 Hz); FTIR (KBr disc, υ_{max}/cm^{-1}): 3182, 2966, 2938, 2878, 1661, 1643, 1575, 1522, 1494, 1460, 1428, 1390,

1347, 1228, 1125, 1060, 957, 842, 719. Elem. Anal: Found: C 60.23, N 8.95, H 6.41%. Calcd for $C_{23}H_{29}N_3O_7$: C60.12, N 9.14, H 6.36%.

N-(3,4,5-Cetyloxybenzoyl)-*N*′-(4′-nitrobenzoyl) hydrazine (C16)

yield 59.5%. δ_H(ppm) (500 MHz; $CDCl_3$; Me_4Si): 9.48 (s, 1H), 9.12 (s, 1H), 8.33 (d, 2H, J = 8.4 Hz), 8.05 (d, 2H, J = 8.4 Hz), 7.04 (s, 2H), 4.01 (dd, 6H, J = 6.1 Hz, J = 12.4 Hz), 1.78 (m, 6H), 1.47 (m, 6H), 1.26 (s, 72H), 0.88 (d, 9H, J = 13.2 Hz); FTIR (KBr disc, υ_{max}/cm^{-1}): 3193, 2922, 2852, 1663, 1593, 1610, 1579, 1494, 1542, 1341, 1467, 1456, 1257, 1232, 1123, 1100, 868, 863, 719. Elem. Anal: Found: C 73.89, N 4.36, H 10.75%. Calcd for $C_{62}H_{107}N_3O_7$: C 73.98, N 4.17, H 10.72%.

N-(3,4,5-Dodecyloxybenzoyl)-*N*′-(4′-nitrobenzoyl) hydrazine (C12)

yield 58.9%. δ_H(ppm) (500 MHz; $CDCl_3$; Me_4Si): 9.69 (s, 1H), 9.22 (s, 1H), 8.30 (d, 2H, J = 8.3 Hz), 8.03 (d, 2H, J = 8.4 Hz), 7.04 (s, 2H), 4.00 (m, 6H), 1.78 (m, 6H), 1.45 (dd, 6H, J = 7.8 Hz, J = 14.2 Hz), 1.26 (s, 24H), 0.88 (t, 9H, J = 6.7 Hz); FTIR (KBr disc, υ_{max}/cm^{-1}): 3193, 2922, 2851, 1662, 1594, 1566, 1610, 1581, 1492, 1525, 1342, 1466, 1456, 1255, 1229, 1123, 1011, 869, 852, 719. Elem. Anal: Found: C 71.35, N 5.17, H 9.89%. Calcd for $C_{50}H_{83}N_3O_7$: C 71.64, N 5.01, H 9.98%.

3,4,5-tris(Hexadecyloxy)-*N*,*N*′-dimethyl-*N*′-(4-nitrobenzoyl) benzohydrazide (Me–C16)

C16 (2.52 g, 2.50 mM) was dissolved in *N*,*N*′-dimethylformamide (100 ml), anhydrous potassium carbonate (6.92 g, 50 mM) and CH_3I (3.55 g, 25 mM) were added. The mixture was stirred under reflux for 3 h. After cooling to room temperature, the reaction mixture was poured into an excess of ice water, and the precipitate recrystallized from anhydrous alcohol; yield 91.5%.

δ_H(ppm) (500 MHz; $CDCl_3$; Me_4Si): 8.26 (d, 2H, J = 7.2 Hz), 7.67 (s, 2H), 6.72 (s, 0.5H), 6.02 (s, 1.5H), 3.84 (m, 6H), 3.37 (d, 3H, J = 10.3 Hz), 3.04 (d, 3H, J = 51.0 Hz), 1.72 (m, 6H), 1.33 (d, 78H, J = 73.3 Hz), 0.88 (t, 9H, J = 6.8 Hz); FTIR (KBr disc, υ_{max}/cm^{-1}): 2956, 2918, 2850, 1677, 1666, 1585, 1529, 1522, 1468, 1427, 1354, 1232, 1124. Elem. Anal: Found: C 74.44, N 3.88, H 11.11%. Calcd for $C_{64}H_{111}N_3O_7$: C 74.30, N 4.06, H 10.81%.

Acknowledgements

The authors are grateful to the National Science Foundation Committee of China (project No. 50373016), Program for New Century Excellent Talents in University of China Ministry of Education, Special Foundation for PhD Program in Universities of China Ministry of Education (Project No. 20050183057) and Project 985-Automotive Engineering of Jilin University for their financial support of this work.

References

1 G. M. Whitesides and B. Grzybowski, *Science*, 2002, **295**, 2418.
2 T. Kato, N. Mizoshita and K. Kanie, *Macromol. Rapid Commun.*, 2001, **22**, 797.
3 D. Demus, J. W. Goodby, G. W. Gray and H. W. Spiess, *Handbook of Liquid Crystals*, Wiley-VCH: Weinheim, 1998.
4 (*a*) M. George and R. G. Weiss, *Chem. Mater.*, 2003, **15**, 2879; (*b*) M. George and R. G. Weiss, *Langmuir*, 2002, **18**, 7124.
5 (*a*) R. Ziessel, G. Pickaert, F. Camerel, B. Donnio, D. Guillon, M. Cesario and T. Prange, *J. Am. Chem. Soc.*, 2004, **126**, 12403; (*b*) M. Hashimoto, S. Ujiie and A. Mori, *Adv. Mater.*, 2003, **15**, 797; (*c*) K. Ohta, M. Moriya, M. Ikejima, H. Hasebe, N. Kobayashi and I. Yamamoto, *Bull. Chem. Soc. Jpn.*, 1997, **70**, 1199–1203; (*d*) K. Yabuuchi and T. Kato, *Mol. Cryst. Liq. Cryst.*, 2005, **441**, 261–273.
6 (*a*) J. H. Jung, G. John, K. Yoshida and T. Shimizu, *J. Am. Chem. Soc.*, 2002, **124**, 10674; (*b*) C. Y. Bao, R. Lu, M. Jin, P. C. Xue, C. H. Tan, T. H. Xu, G. F. Liu and Y. Y. Zhao, *Chem.–Eur. J.*, 2006, **12**, 3287.
7 H. Kobayashi, A. Friggeri, K. Koumoto, M. Amaike, S. Shinkai and D. N. Reinhoudt, *Org. Lett.*, 2002, **4**, 1423.
8 U. Beginn, S. Keinath and M. Möller, *Macromol. Chem. Phys.*, 1998, **199**, 2379.
9 T. Sumiyoshi, K. Nishimura, M. Nakano, T. Handa, Y. Miwa and K. Tomioka, *J. Am. Chem. Soc.*, 2003, **125**, 12137.
10 J. J. V. Gorp, J. A. J. M. Vekemans and E. W. Meijer, *J. Am. Chem. Soc.*, 2002, **124**, 14759.
11 K. Yabuuchi, E. Marfo-Owusu and T. Kato, *Org. Biomol. Chem.*, 2003, **1**, 3464.
12 C. H. Tan, L. H. Su, R. Lu, P. C. Xue, C. Y. Bao, X. L. Liu and Y. Y. Zhao, *J. Mol. Liq.*, 2006, **124**, 32.
13 D. Demus, A. Gloza, H. Hartung, A. Hauser and I. Rapthel, *Cryst. Res. Technol.*, 1981, **16**, 1445.
14 U. Beginn, *Prog. Polym. Sci.*, 2003, **28**, 1049.
15 U. Beginn, G. Lattermann, R. Festag and J. H. Wendorff, *Acta Polym.*, 1996, **47**, 214.
16 D. M. Pang, H. T. Wang and M. Li, *Tetrahedron*, 2005, **61**, 6108.
17 H. T. Wang, B. L. Bai, P. Zhang, B. H. Long, W. J. Tian and M. Li, *Liq. Cryst.*, 2006, **33**, 445.
18 H. T. Wang, D. M. Pang, H. Xin, M. Li, P. Zhang and W. J. Tian, *Liq. Cryst.*, 2006, **33**, 439.
19 X. Zhao, X. Wang, X. Jiang, Y. Chen, Z. Li and G. Chen, *J. Am. Chem. Soc.*, 2003, **125**, 15128.
20 R. B. Martin, *Chem. Rev.*, 1996, **96**, 3043.
21 The assignments of IR absorption bands were based on ref., (*a*) H. Gunzler and H. Gremlich, *IR Spectroscopy*, Wiley-VCH, New York, 2002; (*b*) L. J. Bellamy, in *The Infra-Red Spectra of Complex Molecules*, vol. 1, 3rd ed. Chapman and Hall, London, 1975; (*c*) H. H. Zhang, Y. Q. Wu, B. L. Bai and M. Li, *Spectrochim. Acta, Part A*, 2006, **63**, 117.
22 C. Xue, S. Jin, X. Weng, J. J. Ge and Z. Shen, *Chem. Mater.*, 2004, **16**, 1014.
23 M. Rozenberg, A. Loewenschuss and Y. Marcus, *Phys. Chem. Chem. Phys.*, 2000, **2**, 2699.
24 T. Steiner, *Angew. Chem., Int. Ed.*, 2002, **41**, 48.
25 K. Borisch, S. Diele, P. Göring, H. Kresse and C. Tschierske, *J. Mater. Chem.*, 1998, **8**, 529.
26 D. J. Abdallah and R. G. Weiss, *Langmuir*, 2000, **16**, 352.
27 Y. Hamuro, S. J. Geib and A. D. Hamilton, *J. Am. Chem. Soc.*, 1996, **118**, 7529.
28 M. Suzuki, Y. Nakajima, M. Yumoto, M. Kimura, H. Shirai and K. Hanabusa, *Langmuir*, 2003, **19**, 8622.
29 Y. D. Zhang, K. G. Jespersen, M. Kempe, J. A. Kornfield, S. Barlow, B. Kippelen and S. R. Marder, *Langmuir*, 2003, **19**, 6534.

